

Alteration of superconductivity and radial breathing modes in suspended ropes of carbon nanotubes by organic polymer coatings

M. Ferrier,¹ A. Yu. Kasumov,¹ V. Agache,² L. Buchailot,² A-M. Bonnot,³ C. Naud,³ V. Bouchiat,⁴ R. Deblock,¹ M. Kociak,¹ M. Kobylyko,¹ S. Guéron,¹ and H. Bouchiat¹

¹Laboratoire de Physique des Solides, Associé au CNRS, Université Paris-Sud, 91405 Orsay, France

²Institut d'Electronique, de Microélectronique et de Nanotechnologie, UMR CNRS 8520, Cité Scientifique, Avenue Poincaré, B.P. 69, F-59652 Villeneuve d'Ascq Cedex, France

³Laboratoire d'Etudes des Propriétés Electroniques des Solides, CNRS-Grenoble, Boîte Postale 166, 38042, Grenoble, France

⁴Centre de Recherches sur les Très Basses Températures, CNRS-Grenoble, Boîte Postale 166, 38042, Grenoble, France

(Received 12 September 2006; published 12 December 2006)

We have altered the superconductivity of a suspended rope of single walled carbon nanotubes, by coating it with organic polymers. Upon coating, the normal state resistance of the rope changes by less than 20%. But superconductivity, which on the bare rope shows up as a substantial resistance decrease below 300 mK, is gradually suppressed. We correlate this to the suppression of radial breathing modes, measured with raman spectroscopy on suspended single and double-walled carbon nanotubes. This points to the breathing phonon modes as being responsible for superconductivity in ropes of single walled carbon nanotubes.

DOI: 10.1103/PhysRevB.74.241402

PACS number(s): 74.78.-w, 73.21.-b, 74.40.+k, 78.30.-j

Carbon nanotubes have been heralded as model systems to explore one-dimensional (1D) conductors, in which electron-electron interactions lead to a nonconventional ground state, the Luttinger liquid.¹ In particular, the single particle density of states is depressed at low energy, with a power law whose exponent depends on the interaction strength. The experimental observation of the power law suppression of the tunnel conductance at low energy was therefore interpreted as a proof of this ground state and of the strength of repulsive electron interactions in single walled carbon nanotubes (SWNTs). The discovery of superconductivity in suspended individual ropes of SWNTs therefore was a big surprise.^{2,3} As for doped fullerene molecules,⁴ the question of which phonon modes give rise to the attractive interaction leading to superconductivity is still unsettled. Whereas Sédéki *et al.*⁵ and Gonzalez⁶ consider the coupling to optical phonon modes, De Martino and Egger⁷ conjecture that attractive interactions can be mediated by low energy phonon modes, and specifically the radial breathing modes (RBMs), which are the transverse compression and dilatation modes of carbon nanotubes. They find that the attractive interaction may be strong enough to overcome the repulsive interactions in SWNTs, especially in ropes of SWNTs where the Coulomb interaction can be screened because the SWNTs are packed so closely together. Their theory⁷ also could reproduce the temperature dependence of the superconducting transition observed in ropes.

To experimentally test the role played by the phonon modes on superconductivity, we have gradually coated a suspended rope of SWNTs with organic material. We show that superconductivity is gradually destroyed. Parallel Raman experiments on other samples show that the radial breathing modes are affected by coating, thereby hinting at these modes playing a major role in the superconductivity of carbon nanotubes. The experiments described hereafter also help define the criteria required to observe a superconducting transition in carbon nanotubes.

The sample whose superconductivity we have altered is a

rope containing roughly 40 SWNTs, as determined from its diameter (7 ± 2 nm) measured in a transmission electron microscope (TEM). This rope is produced by arc discharge followed by purification.^{8,9} It is suspended across a $1 \mu\text{m}$ wide slit etched in a suspended silicon nitride membrane, and well connected to nonsuperconducting (normal) electrodes via a nanosoldering technique.³ The electrodes are a trilayer of 5 nm Al_2O_3 , 3 nm Pt, and 200 nm Au deposited in this order on the membrane. The superconducting transition of the uncoated rope was reported in Refs. 2 and 3, and is plotted as curve (a) in Fig. 1. The rope's resistance decreases from 600 Ω above 120 mK to 150 Ω at 25 mK. This transition is weakened in a magnetic field, and suppressed above 0.6 T.

The shot noise power of this rope in the normal state was $S_I = 2eI/120$, much less than the shot noise power $S_I = 2eI/3$ expected for a coherent diffusive sample.^{3,10} Such a large reduction is the sign that transport through the rope is almost ballistic.¹¹ The number of conducting ballistic SWNTs is determined from the normal state resistance, given that the two wire resistance of a SWNT is at least $h/4e^2 \approx 6.5k\Omega$. In the normal state, transport proceeds via ten ballistic tubes. The residual resistance in the superconducting state on the other hand indicates that 40 tubes are superconducting. The increase in the number of effectively conducting tubes as the temperature is lowered is understood in the following manner: in the normal state, selection rules prevent the tunneling of quasiparticles between tubes of different helicity, so that transport occurs only via metallic tubes well connected to the electrodes. Therefore as in the case of the external shell of multiwalled nanotubes, it is likely that the 10 tubes through which current flows in the normal state are those at the circumference of the rope. But in the superconducting state, Cooper pairs can delocalize over all the superconducting tubes since their total momentum is zero.⁶ We have checked that two consecutive cool downs of the bare rope yield a reproducible transition (curves *a* with open symbols in Fig. 1).

The sample was then modified in successive steps. We

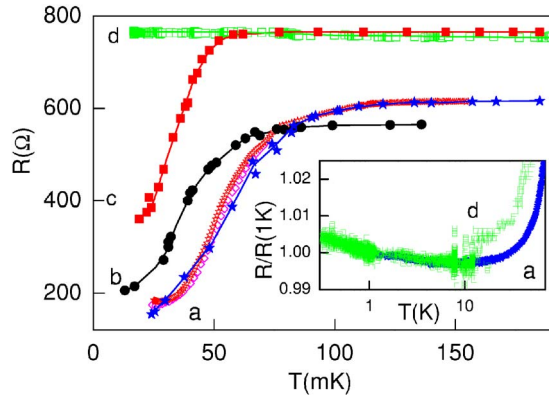


FIG. 1. (Color online) Temperature dependence of the resistance of the 7 nm wide, 1 μm -long rope containing 40 SWNT. (a) Before coating. (b) After benzene-dithiol deposition. (c) After additional coating with PMMA. (d) After completely covering the rope and the slit with PMMA. Lines are guides to the eyes. Curves with full symbols are constructed by extracting the differential conductance at zero current from a $dV/dI(I)$ curve, at different temperatures. This ensures a stable temperature of the sample, which, for reasons which may have to do with the low heat conduction of small superconducting samples, was slow in reaching thermal equilibrium. Curves with open symbols are the recorded differential resistance at zero current as the sample is slowly (a point per minute) heated. The two open symbol curves at stage *a* correspond to two consecutive cool downs of the uncoated sample, and show the reproducibility of the experiment. Inset: Comparison at higher temperature. The upturn in resistance around 10 K is the signature of twiston modes characteristic of well ordered carbon nanotube ropes. Both curves, before and after complete coating are similar, except for the unstable resistance in stage *d* above 10 K.

first (stage *b*) coated it at room temperature with a drop of benzenedithiol. In step *c*, we coated the rope with polymethyl methacrylate (PMMA). In step *d* more PMMA was added, so that the entire slit was covered with PMMA. The trend upon successive coatings, presented in Fig. 1, is to have a slightly modified normal state (high temperature) resistance, which varies between 550 and 750 Ω , and more spectacularly a superconducting transition which weakens as the nanotube rope is coated. The transition temperature T^* , defined as the temperature at which the resistance starts to decrease, which would be the transition temperature of a (hypothetical) corresponding three-dimensional (3D) superconductor, shifts from 120 to 60 mK in curves *a* to *c*. In curve *d*, the coating is so important that no transition is visible down to less than 15 mK. The resistance even increases by 0.5% between 200 and 16 mK.

The gradual weakening of the rope's superconductivity is even more clearly seen in the differential resistance curves plotted in Fig. 2. The differential resistance of the uncoated rope (curve *a*) is typical of a 1D superconductor¹² (a wire in which the superconducting coherence length is larger than the diameter): the differential resistance is smallest at zero current bias, and increases with jumps and peaks typical of phase slips¹³ as the current through the rope is increased. At high current bias, the normal state resistance is recovered. We define a critical current I_c as the current above which the differential resistance jumps from a low value to a high value

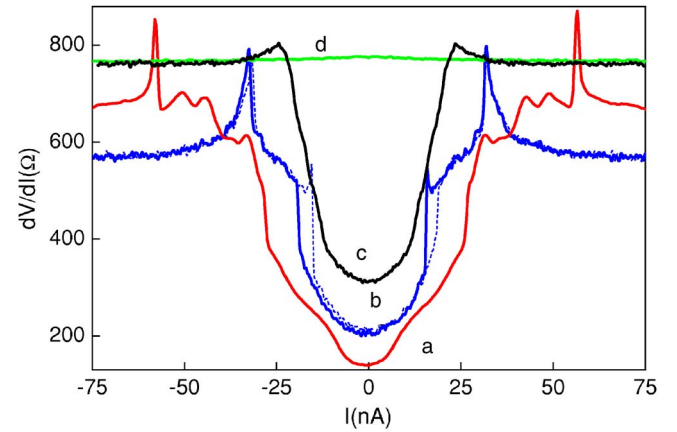


FIG. 2. (Color online) Differential resistance of the nanotube rope at stages *a* through *d*. Curve *a* was taken at 28 mK with an ac excitation of 1 nA, curve *b* at 14 mK with $i_{ac}=0.1$ nA, curve *c* at 15 mK with $i_{ac}=0.1$ nA, and curve *d* at 15 mK with $i_{ac}=1$ nA. Both the up (dashed) and down current sweep directions are plotted for curve *b*, illustrating the asymmetry of these current-biased curves.

(in analogy to the bulk critical current, at which the differential resistance jumps from zero to finite resistance). We also define I_c^* as the current of the last resistance peak, above which all traces of superconductivity disappear. As shown on the example of curve *b*, the $dV/dI(I)$ curves are hysteretic, and we take the largest values to be the critical values. They are given in Table I for successive coatings, and are seen to decrease as the rope is coated with an increasing amount of organic material. Note that two successive cool downs of the uncoated rope give identical differential resistance curves within 10% (not shown).

The resistance variations with magnetic field are shown in Fig. 3. No qualitative difference is noticeable between curves *a*, *b*, and *c*, which show a large (more than 50%) positive magnetoresistance (the resistance increases as the magnetic field destroys superconductivity). The amplitude of this magnetoresistance decreases as the temperature is increased, but persists up to 1 K, which is nearly $10 T^*$. The critical field, above which the differential resistances do not show a dip at low current, is 0.6 T. Interestingly, a small (0.5%) positive magnetoresistance is visible at stage *d*, where no other trace of superconductivity is measurable, and has an amplitude

TABLE I. Rope characteristics at different modification stages. The rope contains roughly 40 nanotubes and is 1 μm long. *a*: Before coating, as reported in Ref. 3; *b*: After coating with benzenedithiol; *c*: After further coating with PMMA; *d*: Additional PMMA. I_c and I_c^* are the currents at which the first and last differential resistance jumps occur.

	R_{1K}	T^*	I_c	I_c^*
$R4a_{\text{PtAu}}$	627 Ω	120 mK	28 nA	58 nA
$R4b_{\text{PtAu}}$	564 Ω	80 mK	19 nA	32 nA
$R4c_{\text{PtAu}}$	763 Ω	60 mK	0 nA	24 nA
$R4d_{\text{PtAu}}$	767 Ω	<15 mK	0 nA	0 nA

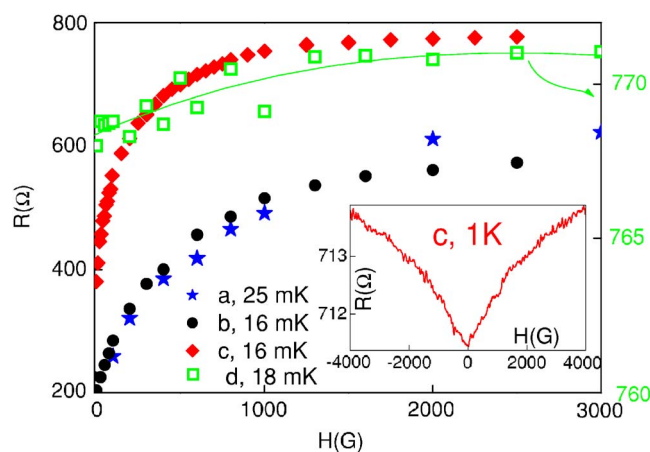


FIG. 3. (Color online) Magnetoresistance at the different coating stages. A large positive magnetoresistance is seen at low temperature for stages *a*, *b*, and *c*. At stage *d* the magnetoresistance is still positive, but small (0.1%), identical to the magnetoresistance of stage *c* at 1 K (inset). Left resistance scale: Stages *a*, *b*, and *c* at low temperature. Right resistance scale is relative to stage *d* that shows a very small positive magnetoresistance. The line is a guide to the eye.

similar to the magnetoresistance of stage *c* at 1 K, as shown in the inset of Fig. 3. Superconducting fluctuations over such broad temperature ranges are typical of low dimensional superconductivity.

To understand the link between the weakening of superconductivity and the effect of coating on the phonon modes of these ropes, we have investigated the effect of PMMA deposition on the Raman response of other suspended nanotubes. The nanotubes grown for this purpose were synthesized by chemical vapor deposition (CVD),¹⁴ and were also suspended across a slit in a nitride membrane. Figure 4 shows an image of carbon nanotubes grown in this manner. TEM and Raman investigations show that the nanotubes are single- and double-walled carbon nanotubes (mostly SWNT), sometimes assembled in small ropes of at most ten tubes. Resonant Raman measurements are performed using the 1.96 eV radiation of a 633 nm He-Ne laser with a $1 \mu\text{m}^2$ spot size, so that only a few suspended tubes are in resonance with the laser. Typical Raman spectra [see Fig. 4(a)] contain RBM in the $100\text{--}260 \text{ cm}^{-1}$ wavelength range (12.5 to 32.4 meV, which, given the theoretical law of $27.8/d \text{ meV}$,¹⁵ where d is the SWNT diameter in nm, corresponds to diameters between 0.9 and 2.2 nm), and tangential modes around $1560\text{--}1600 \text{ cm}^{-1}$. The low Raman signal intensity, along with the observation of one or two RBM point to the presence of single isolated tubes or just a few SWNTs.¹⁶ Also, the low intensity of the band at 1320 cm^{-1} which characterizes structural disorder suggests that these tubes are relatively defect free. The 218 cm^{-1} frequency of Fig. 4 is typical of the Raman resonant RBM of metallic tubes.¹⁷ The broad asymmetric tangential band around 1530 cm^{-1} is the signature of the Breit Wigner Fano electron-phonon intertube interaction specific to metallic nanotubes,¹⁸ while the sharper peak at 1590 cm^{-1} is typical of tangential modes.

Figure 4 shows the evolution of phonon modes with coat-

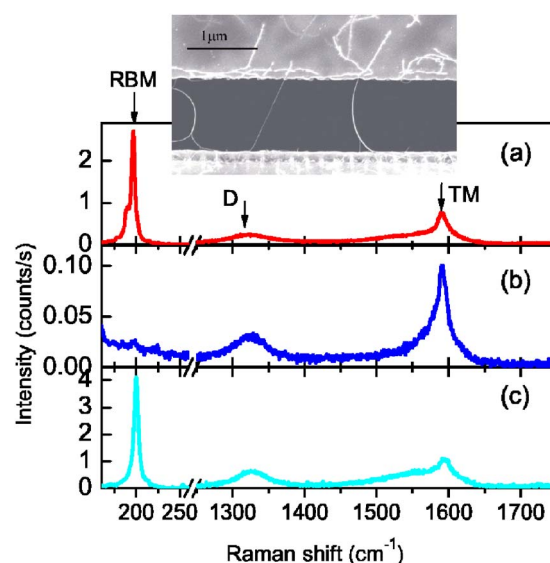


FIG. 4. (Color online) Influence of PMMA on the Raman spectra of suspended SWNTs. Raman spectra obtained at room temperature with a He-Ne laser of probe area roughly $1 \mu\text{m}^2$. Raman spectra before deposition (a), after deposition (b), and after removal of PMMA in acetone (c). The spectra are of different parts of the sample, chosen because of their similar frequencies (see text). RBM, *D*, and *T*, respectively, stand for radial breathing mode, disordered graphite mode, tangential modes. Inset: field emission scanning electron micrograph of a typical sample of CVD-grown tubes.

ing by comparing Raman spectra before (a) and after (b) PMMA deposition, and after removal of PMMA in acetone (c). Although these spectra do not correspond to the very same tubes, because of the absence of precise sample repositioning, the tubes are nonetheless of roughly the same diameter, since the RBM have the same frequency. Since coating with PMMA decreases the overall Raman signal, we compare the *relative* intensity of the RBM with respect to the tangential modes (TM). In the uncoated sample [spectrum (a)], the intensity of the RBM peak is much greater than the intensity of the TM. This is due to the fact that the tubes are suspended, and therefore do not interact through Van der Waals interaction with the substrate.¹⁹ With coating we find that the RBM intensity becomes much smaller (at least an order of magnitude) than the intensity of the TM. After removal of the PMMA with acetone, the overall Raman intensity is recovered, as is the large intensity of the metallic RBM relative to the TM. The spectra and ratios of Fig. 4 are typical of what we find in many measurements on this sample and others.²⁰

The fact that the absolute RBM signal is much larger for suspended tubes than for tubes on a substrate has also been observed in recent scanning tunneling microscopy experiments on suspended nanotubes.²¹ The authors found spectroscopic signature of the RBM modes only on the suspended portions of the tubes, and not on the contact regions. However, our experiment also shows that coating tubes with PMMA suppresses their RBM much more than the TM. In the transport experiment on the rope containing 40 tubes, it is therefore likely that the RBM of the tubes on the surface of the rope are suppressed because they are coated by PMMA.

The disappearance of superconductivity could therefore be explained by the fact that the blocking of the RBM of the 10 connected outer tubes causes the suppression of their superconducting transition. Although the inner tubes which are uncoated by PMMA could still be superconducting, the superconducting transition would not be seen in a transport experiment since there is barely any electronic transfer between normal external tubes and inner tubes.⁶

Interestingly, although the RBM are clearly suppressed in the coated rope, it seems as though the twiston modes are not affected. Twistons, the long-wavelength torsional modes of nanotubes, are known to backscatter electrons efficiently, as demonstrated by a measurable linear temperature dependence down to 100–10 K, below which a resistance increase takes place.²² As shown in Fig. 1, before coating and after complete coating, the resistance decrease and upturn with decreasing temperature are similar, suggesting that the twiston modes are not modified by coating, as expected for optical modes. This experiment therefore seems to confirm the theoretical picture put forth in Ref. 7 that the RBM more than the longitudinal modes cause superconductivity. The twiston modes backscatter electrons efficiently but do not participate in the phonon-induced forward scattering of electrons responsible for the attractive interaction.

We argue that the progressive destruction of superconductivity is not due to an increase of disorder in the sample, for several reasons. The first is the small relative resistance

change (less than 1%) between stage *c* and *d*, which shows that disorder is not qualitatively different. The destruction of superconductivity in stage *d* is therefore caused by some other mechanism. For the same reason, the destruction of superconductivity cannot be attributed to a pressure-induced modification of the nanotubes' band structures, turning metallic tubes into semiconducting ones, for this would change by a large amount the sample resistance. Lastly, very low shot noise was found in stages *a* and *c*, indicating that transport remains ballistic as polymer is added.

We have shown that coating nanotubes with polymers suppresses the radial breathing modes of individual SWNTs, and suppresses the superconducting transition of a rope of 40 SWNTs. This suggests that the RBM play a role in the superconductivity of carbon nanotubes. The experiments conducted down to low temperature to this day outline the stringent requirements to observe superconductivity: nanotubes should not be coated by polymers, and should be suspended. They should be long enough in order to avoid the inverse proximity effect, which causes the proximity to normal contacts to destroy the superconductivity in the tubes. Finally, there should be efficient screening of the repulsive interaction in nanotubes, so that superconductivity should develop most in tubes that are assembled in a rope.

We thank C. Pasquier for useful input and M. Potemski for additional Raman measurements.

- ¹R. Egger and A. O. Gogolin, *Phys. Rev. Lett.* **79**, 5082 (1997).
²M. Kociak *et al.*, *Phys. Rev. Lett.* **86**, 2416 (2001); Superconducting fluctuations were subsequently observed in individual SWNT: Z. K. Tang *et al.*, *Science* **292**, 2462 (2001); J. Zhang *et al.*, *Phys. Rev. B* **74**, 155414 (2006), and in multiwall carbon nanotubes, I. Takesue *et al.*, *Phys. Rev. Lett.* **96**, 057001 (2006).
³A. Kasumov *et al.*, *Phys. Rev. B* **68**, 214521 (2003).
⁴M. S. Dresselhaus, G. Dresselhaus, and P. C. Eklund, *Science of Fullerenes and Carbon Nanotubes* (Academic Press, San Diego, 1995).
⁵A. Sédéki, L. G. Caron, and C. Bourbonnais, *Phys. Rev. B* **65**, 140515(R) (2002).
⁶J. Gonzalez, *Phys. Rev. Lett.* **87**, 136401 (2001); **88**, 076403 (2002); *Phys. Rev. B* **67**, 014528 (2003).
⁷A. De Martino and R. Egger, *Phys. Rev. B* **67**, 235418 (2003); **70**, 014508 (2004); M. Ferrier *et al.*, *Solid State Commun.* **131**, 615 (2004).
⁸C. Journet *et al.*, *Nature (London)* **388**, 756 (1997).
⁹L. Vaccarini *et al.*, *C. R. Acad. Sci.* 327, 925 (1999).
¹⁰M. Ferrier, Ph.D. thesis, Université Paris 11, Paris, 2004.
¹¹P.-E. Roche *et al.*, *Eur. Phys. J. B* **28**, 217 (2002); *Proc. SPIE*

- 5115**, 104 (2003).
¹²A. Rogachev and A. Bezryadin, *Appl. Phys. Lett.* **83**, 512 (2003).
¹³N. Giordano, *Phys. Rev. B* **41**, 6350 (1990).
¹⁴L. Marty *et al.*, *Nano Lett.* **3**, 1115 (2003); A. Iaia *et al.*, *Thin Solid Films* **501**, 221 (2006).
¹⁵M. J. Dresselhaus and P. C. Eklund, *Adv. Phys.* **49**, 705 (2000); A. Jorio *et al.*, *Phys. Rev. B* **65**, 155412 (2002).
¹⁶M. S. Dresselhaus *et al.*, *Carbon* **40**, 2043 (2002).
¹⁷H. Kataura *et al.*, *Synth. Met.* **103**, 2555 (1999).
¹⁸C. Jiang *et al.*, *Phys. Rev. B* **66**, 161404(R) (2002).
¹⁹L. Marty, Ph.D. thesis, Université J. Fourier, Grenoble I, 2004.
²⁰The same Raman experiments performed on large ropes of the same batch as measured in the transport experiment (containing about 100 tubes) did not show a significant reduction of the RBM relative intensity upon coating with PMMA. This is expected given that in such large ropes the Raman signal comes from the more numerous inner (uncoated) tubes. This shows that only the RBM of the outer tubes are modified.
²¹B. J. LeRoey, S. G. Lemay, J. Kong, and C. Dekker, *Nature (London)* **432**, 371 (2005); *Appl. Phys. Lett.* **84**, 4280 (2004).
²²C. L. Kane *et al.*, *Europhys. Lett.* **41**, 683 (1998).